Expression of NF-L in both Neuronal and Nonneuronal Cells of Transgenic Mice: Increased Neurofilament Density in Axons without Affecting Caliber

Mervyn J. Monteiro,* Paul N. Hoffman,§ John D. Gearhart,‡ and Don W. Cleveland*

Departments of *Biological Chemistry, ‡Physiology, and §Ophthalmology and Neurology, The Johns Hopkins University School of Medicine, Baltimore, Maryland 21205

Abstract. We have generated transgenic mice containing additional copies of the murine NF-L gene in order to examine the consequences of neurofilament-L overexpression on axonal morphology. Founder mice were constructed to carry a transgene in which the presumptive 5' promoter sequences of NF-L were replaced with the strong murine sarcoma virus long terminal repeat promoter. The transgenes were expressed prominently in several tissues, including skeletal muscle and kidney where NF-L accumulated to ~2% of cell protein. This was not accompanied by an overt phenotype, except that expression in lens led to cataract formation. In the brains of these animals, transgene RNA levels exceeded the endogenous NF-L RNAs by up to 20-fold, although no additional protein accumulated, indicating posttranscriptional regulation of NF-L expression. However, in peripheral neurons transgene RNA was approximately fourfold higher than endogenous NF-L mRNAs, and a corresponding increase in NF-L subunits was found in axons arising from these neurons. Myelinated nerve fibers of transgenic animals contained increased numbers of NFs, assembled predominantly of NF-L. This was reflected in an increase in the density of axonal NFs; axonal caliber was not affected.

NTERMEDIATE filaments (IFs)[1] are 10-nm filaments which, together with microtubules and microfilaments, form the cytoskeleton of eukaryotic cells. However, unlike microtubules and microfilaments whose subunits are well conserved in sequence, IFs from different tissues are assembled from a more divergent subunit composition. This heterogeneity has been shown by biochemical, immunological, and molecular characterization to be due principally to differences in the "head" and "tail" domains of the subunit polypeptides which otherwise all contain a central, structurally conserved, α-helical coiled-coil domain of ~310 residues (Geisler and Weber, 1986; Franke, 1987; Steinert and Roop, 1988). On the basis of sequence differences and on the conservation of the intron positions, IFs have been divided into five generally accepted classes. Class I and class II are composed of the type I (acidic) and type II (basic) keratins, respectively, both of which are expressed in epithelial cells. Class III consists of vimentin expressed in mesenchymal cells, desmin expressed in muscle cells, glial fibrillary acid

protein expressed in glial cells, and peripherin expressed in a subset of neurons of the peripheral nervous system. Class IV comprises the major neurofilament (NF) proteins that are probably expressed in all neuronal cells. Class V comprises the nuclear lamins. The newly discovered IF subunit nestin, found in neuroepithelial stem cells, has been proposed to represent a separate sixth IF class (Lendahl et al., 1990).

In mammals, NFs are composed primarily of three subunits, NF-L (68 kD), NF-M (160 kD), and NF-H (200 kD) (Hoffman and Lasek, 1975). Each carries a 310–amino acid α-helical rod domain following an ~100-residue head domain, and differences in size are primarily due to the length of the carboxy-terminal tail sequences (Lewis and Cowan, 1986; Levy et al., 1987; Myers et al., 1987; Julien et al., 1988; Lees et al., 1988). The disposition of the three NF proteins in the native polymer is not known; however, since all three subunits contain the rod domain, almost certainly each is an integral filament subunit. The role of head and tail domains is less clear but immunocytochemical and in vitro reassembly experiments suggest that the tail domains of NF-M and NF-H are mostly involved in the formation of NF cross-bridges (Geisler and Weber, 1981; Sharp et al., 1982; Geisler et al., 1983; Julien and Mushynski, 1983; Minami and Sakai, 1985; Hirokawa et al., 1984; Hisanaga and Hirokawa, 1988).

A convincing functional role for any IF has yet to be

1. *Abbreviations used in this paper:* DRG, dorsal root ganglia; IF, intermediate filament; LTR, long terminal repeat; MSV, murine sarcoma virus; NF, neurofilament.
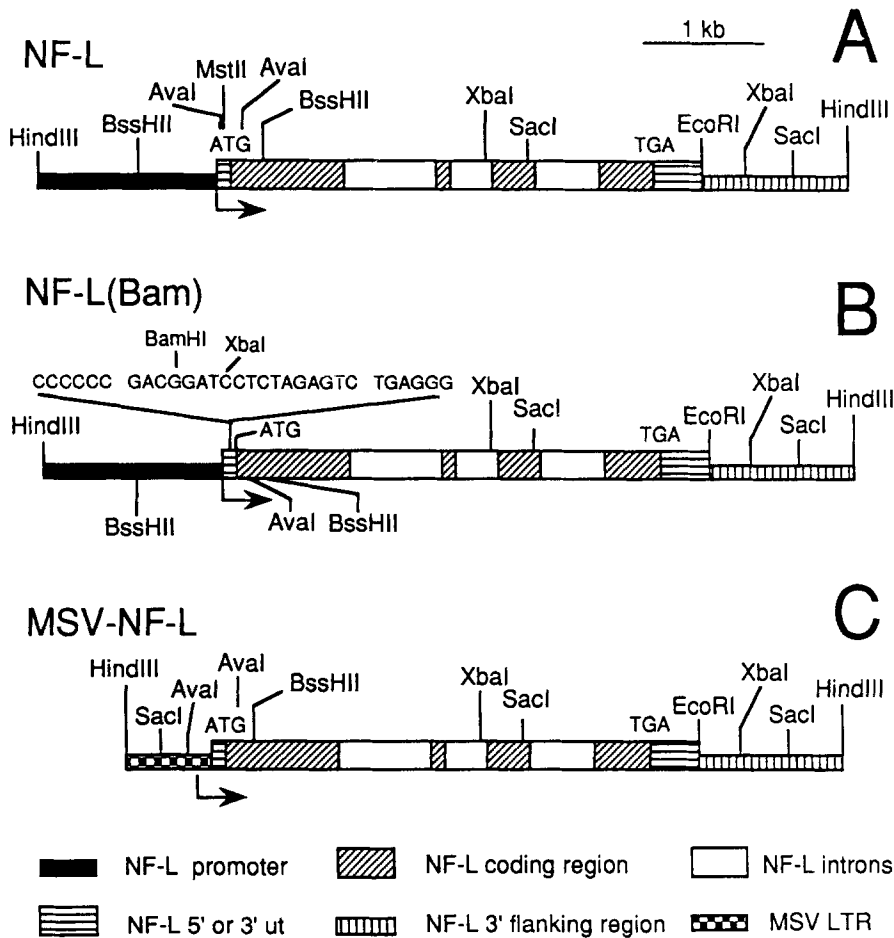
Figure 1. Schematic drawings of the mouse NF-L gene and the two NF-L transgene constructs. (*A*) Restriction map and principal features of the 7-kb Hind III fragment containing the mouse NF-L gene. (*B*) Schematic drawing of pNF-L(Bam). This gene was constructed by inserting a 18-bp sequence, containing Bam HI and Xba I restriction sites, between the Ava I and Mst II sites of pNF-L (5 bases were deleted in this process leaving a net insertion of 13 bp). (*C*) Schematic drawing of pMSV-NF-L. This gene was constructed by replacing the 5' 1.7-kb Hind III–Bam HI fragment of pNF-L(Bam) with the 0.6-kb Hind III–Bgl I fragment that contains the MSV promoter segment.

proven, although the keratin and lamin networks are almost certainly required for structural integrity of the epidermis and nuclear lamina, respectively. For NFs, a functional role was first suggested on the basis of the close correlation between the number of axonal NFs and the cross-sectional areas of large myelinated nerve fibers (Friede and Samorajski, 1970; Weiss and Mayr, 1971; Berthold, 1978). More direct evidence for a role of NFs in the control of axonal caliber was provided by the observation that reductions in NF gene expression after axotomy correlate with somatofugal axonal atrophy (Hoffman et al., 1987). This axonal atrophy, which is associated with reductions in both the amount of pulse-labeled NF protein undergoing axonal transport in the proximal stumps of transected nerve fibers and axonal NF content, begins proximally near the cell body (soma) and spreads somatofugally along the nerve fiber at a rate equal to the velocity of NF transport along the axon (Hoffman et al., 1984; 1985). Additional evidence for the role of NFs in the control of caliber comes from recent studies which show that the radial growth of myelinated nerve fibers, which occurs during postnatal development, correlates temporally with the induction of NF gene expression in developing sensory neurons (Muma, N. A., and P. N. Hoffman, unpublished observations).
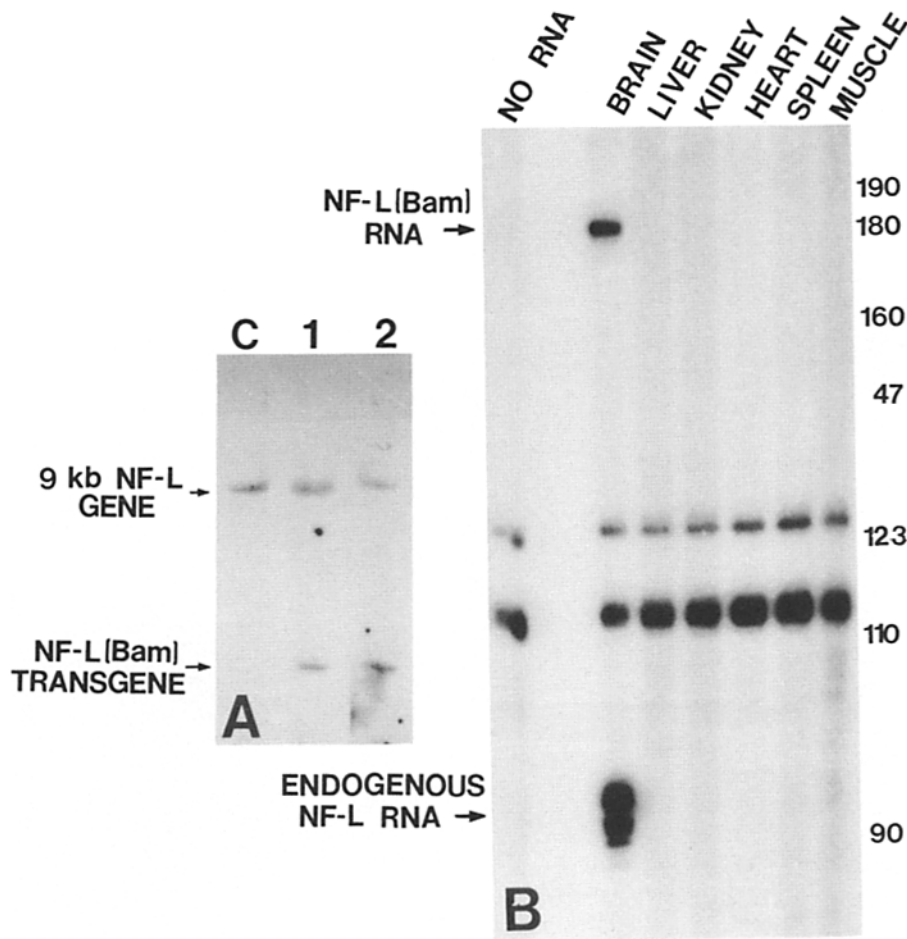
NF-L is the most abundant NF subunit and in vitro experiments have shown it to be capable of assembly without the other subunits (Geisler and Weber, 1981; Liem and Hutchin-

son, 1982). We previously demonstrated that forced expression of NF-L in fibroblasts resulted in the assembly of the protein into filaments and was not detrimental to the growth of fibroblasts (Monteiro and Cleveland, 1989). However, it was not known if similar high levels of inappropriate expression of an IF would affect embryogenesis or development. To begin to address such questions, including the role of each NF subunit in neuronal function, we have generated transgenic mice expressing high levels of NF-L in both neuronal and nonneuronal cell types. The resultant increased expression and assembly of NF-L in neurons allowed us a first test of the hypothesis that NF expression is an intrinsic determinant of axonal caliber. We show that increased NF-L expression alone is in fact not sufficient to affect axonal caliber; rather, it generates disorganization of the NF array in axons.

Materials and Methods

Molecular Cloning of the Mouse pNF-L Gene: Construction of pNF-L(Bam) and pMSV-NF-L Transgenes

As described previously, the complete NF-L gene of mouse was isolated as a 7-kb Hind III fragment, and subcloned into pUC9 to yield pNF-L (Monteiro and Cleveland, 1989). For transgenic animals, pNF-L was manipulated to produce two additional clones, pNF-L(Bam) and pMSV-NF-L (Fig. 1). pNF-L(Bam) contains the entire NF-L coding sequences including 1.7 kb of sequences 5' to the ATG start codon and 1.7 kb of 3' terminal noncod-

ing sequences. This clone differs from the authentic gene by insertion of an 18-base linker sequence at the abutting Ava I–Mst II sites in the 5' untranslated region, resulting in the loss of 5 NF-L nucleotides but a net gain of 13 nucleotides. Using S1 nuclease protection methods, transcripts derived from pNF-L(Bam) can be distinguished from authentic NF-L RNAs by the presence of the linker sequence (Monteiro and Cleveland, 1989). pMSV-NF-L was constructed by replacing the Hind III–Bam HI fragment of pNF-L(Bam) with a 0.6-kb Hind III–Bgl II fragment containing the murine sarcoma virus (MSV) long terminal repeat (LTR) (Fig. 1 C; see also Monteiro and Cleveland, 1989).

Production of Transgenic Mice

Embryos were recovered from the oviducts of superovulated B6AF$_1$J females ∼12 h after fertilization. The female pronucleus of one-cell embryos was injected with ∼300 copies of DNA fragments containing either the 7-kb Hind III fragment of the pNF-L(Bam) gene construct (Fig. 1 B) or with 5.9-kb Hind III fragment of pMSV-NF-L (Fig. 1 C). The DNA fragments were gel purified from vector sequences using DEAE paper (Dretzen et al., 1981). After incubation at 37°C for 18 h in Whitten's medium, the surviving two-cell embryos were transferred to the oviducts of pseudopregnant CD1 females. Mice born from these mothers were analyzed for the presence of the transgenes as described below.

Southern Blotting of Mouse Tail DNA

Transgenic mice were identified by screening DNA isolated from mouse tail for the presence of the injected DNA fragments. 3 wk after birth a portion of the mouse tail was excised with a razor blade, and the tissue dispersed with a polytron homogenizer into 10 ml of 10 mM Tris-HCl, pH 7.5, 100 mM NaCl, 1 mM sodium EDTA. The samples were incubated at 37°C for

1 h after addition of Sarkosyl to 1% (wt/vol), pronase to 200 μg/ml, and RNase A to 100 μg/ml. The DNA was extracted once with phenol/chloroform (1:1), once with ether, then adjusted to 0.3 M with potassium acetate and precipitated at −20°C with 2 vol ethanol. The DNA precipitate was collected by centrifugation, resuspended in 10 mM Tris-HCl, 1 mM sodium EDTA, and a 10-μg aliquot was cleaved with restriction enzymes (Eco RI and Bam HI for analysis of the pNF-L[Bam] transgene and with Sac I for the analysis of the pMSV-NF-L transgene), separated by agarose gel electrophoresis, and transferred onto nitrocellulose paper (Southern, 1975). The nitrocellulose was baked at 80°C for 1 h; prehybridized at 42°C in 50% formamide, 5× SSC (1× SSC is 0.15 M NaCl, 0.015 M sodium citrate, pH 7.0), 50 mM Tris-HCl, pH 7.5, 0.5% (wt/vol) SDS, 1 mM sodium EDTA, 5× Denhardt's solution (Denhardt, 1966), and 100 μg/ml of sonicated, denatured salmon sperm DNA; and then hybridized for 48 h with 1 × 10^6 cpm/ml of labeled probe prepared by random primer extension using radioactive α-^{32}P-dATP and AMV reverse transcriptase. For detection of the pNF-L(Bam) transgene, the probe was the 4.2-kb Bam HI–Eco RI fragment of pNF-L(Bam) (Fig. 1 B).

SDS-PAGE and Immunoblot Detection of NF-L in Tissue Samples

Mouse tissues were lysed in 0.5% (wt/vol) SDS, 50 mM Tris-HCl, pH 6.8, 8 M urea, then boiled in Laemmli loading buffer (Laemmli, 1970) containing 2% β-mercaptoethanol, and the proteins were separated by electrophoresis on 6 or 8.5% polyacrylamide gels (Laemmli, 1970). Proteins were transferred onto nitrocellulose filters (type BA83; Schleicher and Schuell, Inc., Keene, NH) and immunoblotted as described by Lopata and Cleveland (1987). NF-L protein was detected by autoradiography by incubating the filters first with the mouse monoclonal anti–NF-68 antibody (Boehringer
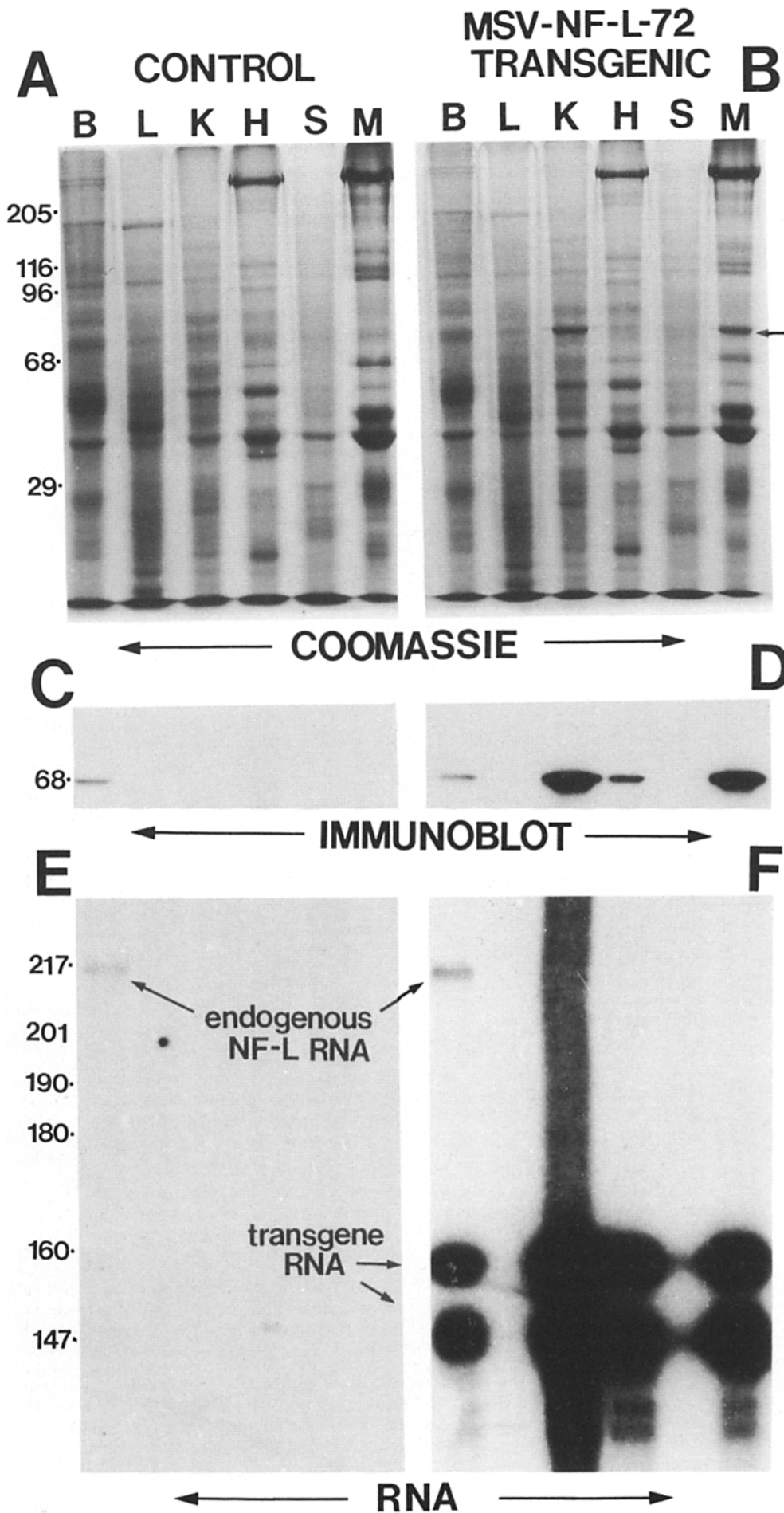
Figure 3. pMSV-NF-L transgenic mice express high levels of NF-L in many different tissues. (*A* and *B*) Coomassie blue–stained gels of tissue extracts (40 μg of protein analyzed per lane) from different tissues of a control and a transgenic mouse (MSV-NF-L-72). The tissue samples analyzed were (*B*) brain, (*L*) liver, (*K*) kidney, (*H*) heart, (*S*) spleen, and (*M*) muscle. The gels were calibrated using protein molecular mass markers (shown in kD). The arrow marks the position of a novel protein found in kidney and muscle of transgenic animals. (*C* and *D*) Immunoblot of parallel gels using an NF-L–specific antibody. (*E* and *F*) S1 nuclease protection analyses of the accumulated NF-L RNAs in different tissues of a transgenic mouse (MSV-NF-L-72). RNA was isolated from the tissues shown and 10-μg aliquots were analyzed for NF-L RNAs using the Ava I–Ava I fragment of the wild-type NF-L gene (end-labeled with ^{32}P) as the probe. S1-resistant products at 215 bases map to the start of transcription of the endogenous NF-L and those at position 145–158 b report transgene NF-L RNAs. (*E*) RNA from control mouse; (*F*) RNA from MSV-NF-L-72 transgenic mouse. Markers (shown in nucleotides) were Hpa II DNA fragments of pBR322.
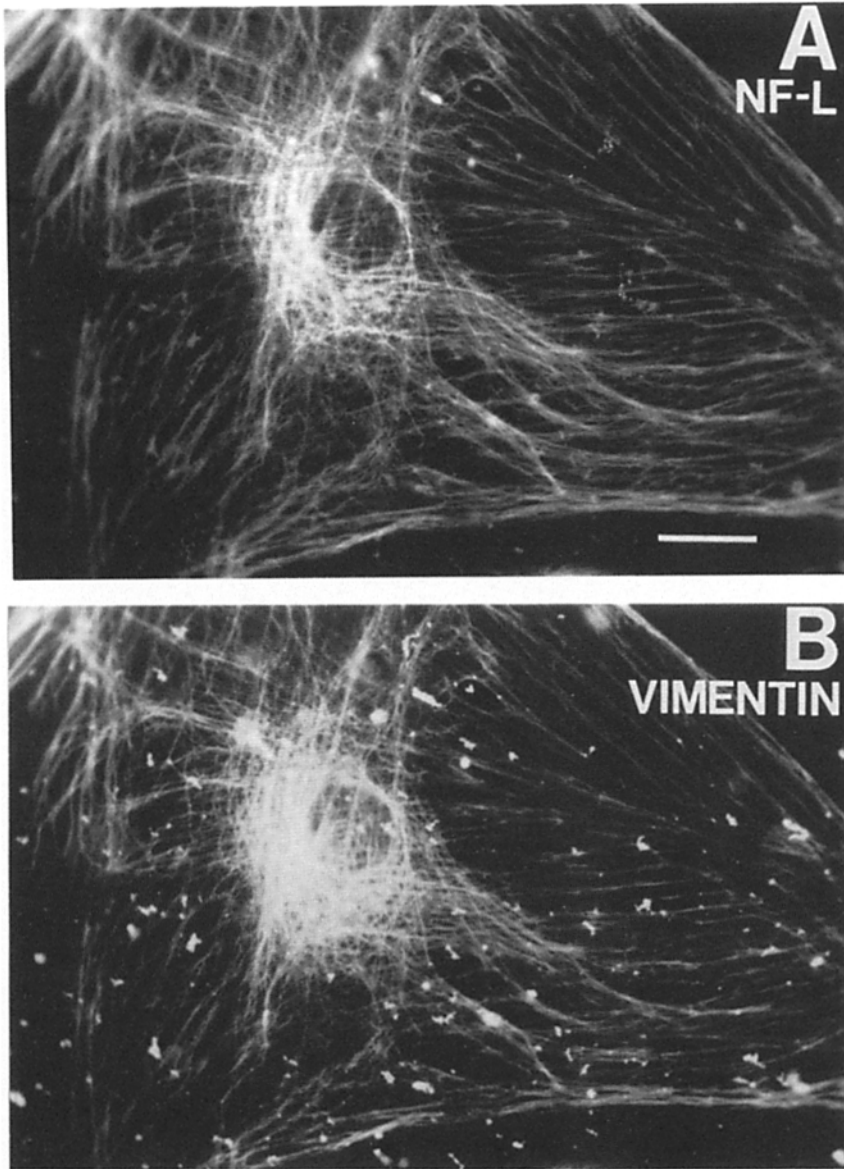
Figure 4. Assembly of NF-L in primary cultures of transgenic fibroblasts. Primary fibroblasts from mouse embryos of line MSV-NF-L-58 were stained in *A* for NF-L using a commercially available monoclonal antibody to murine NF-L and a secondary antibody coupled to fluorescein. (*B*) Vimentin filaments were localized simultaneously using a rabbit polyclonal antibody to vimentin and a rhodamine-linked anti–rabbit antibody. Bar, 20 μm.

Mannheim Diagnostics, Inc., Houston, TX) followed by ^{125}I-labeled sheep anti–mouse antibody (Amersham Corp., Arlington Heights, IL).

RNA Isolation and S1 Nuclease Protection of mRNA

NF-L expression in mouse tissues was examined by S1 nuclease protection of mRNA. Total RNA was isolated from mouse tissue by the guanidinium isothiocyanate/cesium chloride method (Chirgwin et al., 1979). To analyze for accumulation of the pNF-L(Bam) transgene RNAs, the 1.9-kb Hind III–Ava I fragment of pNF-L(Bam) (Fig. 1 *B*) was gel purified, 5' end-labeled with γ-^{32}P-dATP using T4 polynucleotide kinase and hybridized to 5 or 10 μg of total RNA for 18 h at 52°C. Analysis for expression of the pMSV-NF-L transgene was performed with 5' end-labeled probes from the 340-bp Ava I–Ava I of pMSV-NF-L or the 1-kb Bss HII fragment of pNF-L. RNA/DNA hybrids were precipitated with ethanol and treated for 1 h at room temperature with 100 U of S1 nuclease in 100 μl of 0.25 M NaCl, 30 mM sodium acetate, 5 mM ZnCl₂, and 7.5 μg sonicated, denatured salmon sperm DNA. The S1-resistant radioactive products were separated by electrophoresis through a 6% polyacrylamide, 8 M urea gel and identified by autoradiography. The size of the protected fragments was determined by comparison with the mobilities of ^{32}P-labeled fragments of Hpa II–digested pBR322.

Immunofluorescence Microscopy of Transgenic Fibroblasts

Cultures of fibroblastic cells were prepared from adult (3-mo-old) transgenic or control mice by mincing sections of thigh muscle with a razor blade, followed by brief trypsinization. The resultant cell suspension was plated onto plastic culture dishes and grown for 2 wk in DME plus 10% FCS. Media were changed every 3 d. This yielded a population of remaining cells that was enriched in fibroblasts.

For immunofluorescence, cells were trypsinized and plated onto glass coverslips. For visualization of NF and vimentin arrays, cells were washed for 30 s at room temperature in 4 M glycerol, 100 mM Pipes, pH 6.9, and 1 mM EGTA, and then extracted for 30 s in the same solution containing 0.5% Triton X-100. The first wash was repeated and the samples were fixed in −20°C methanol for 5 min. The samples were rehydrated in PBS and incubated with an antibody solution (containing PBS supplemented with 1% nonfat dry milk) for 1 h at room temperature. After a similar incubation with a solution containing secondary antibodies, the coverslips were washed in PBS and mounted on glass slides using Aqua-mount (Lerner Laboratories, New Haven, CT). Cells were examined on an Olympus BH-2 microscope using epifluorescence optics and photographed on TMAX film (Eastman Kodak Co., Rochester, NY). Primary antibodies used were a mouse mAb to NF-L (Boehringer Mannheim Biochemicals, Indianapolis, IN) and
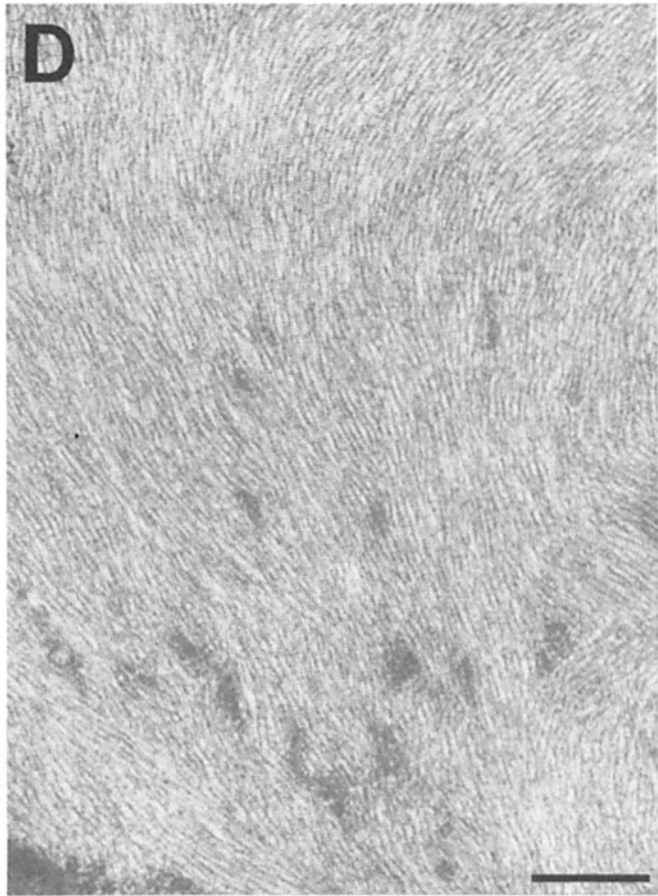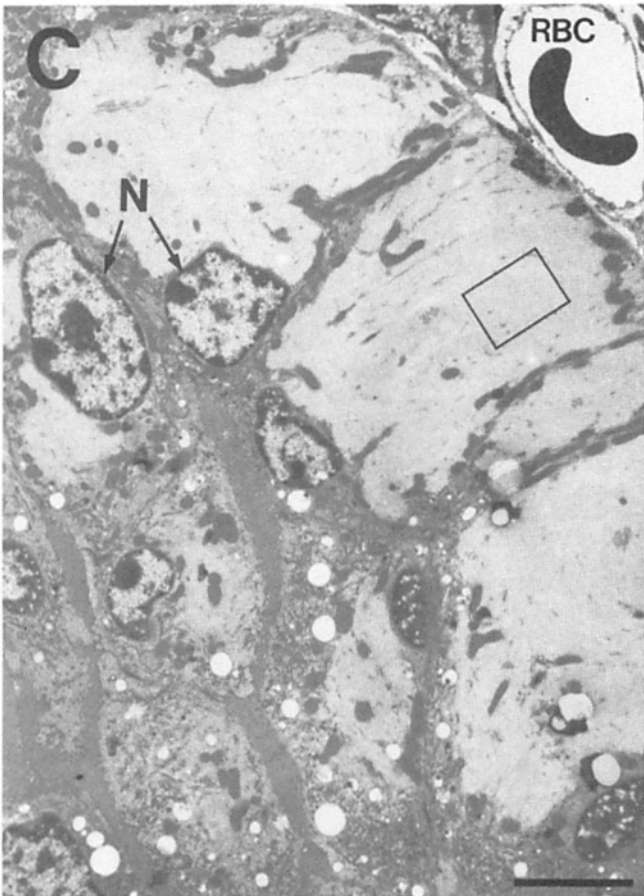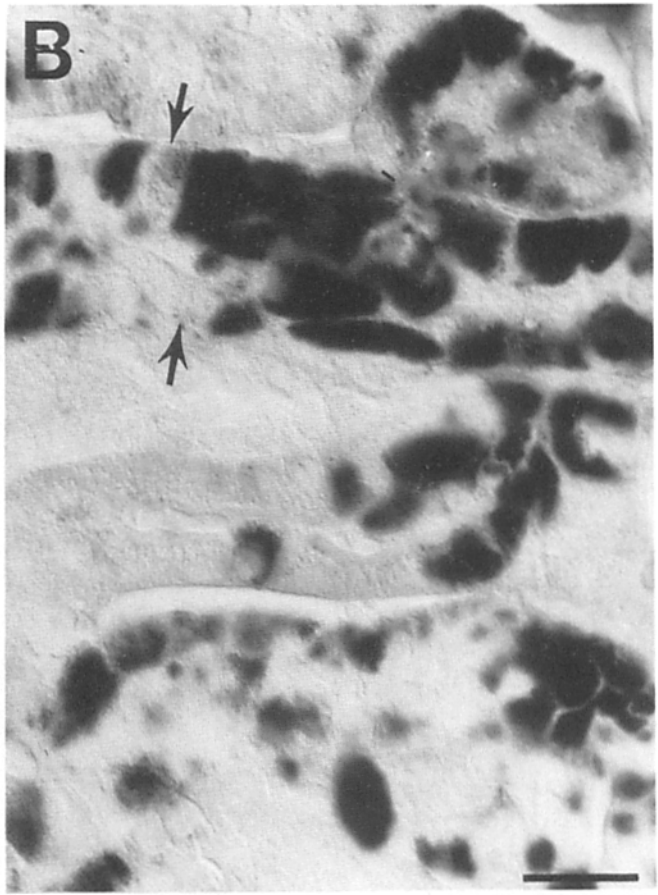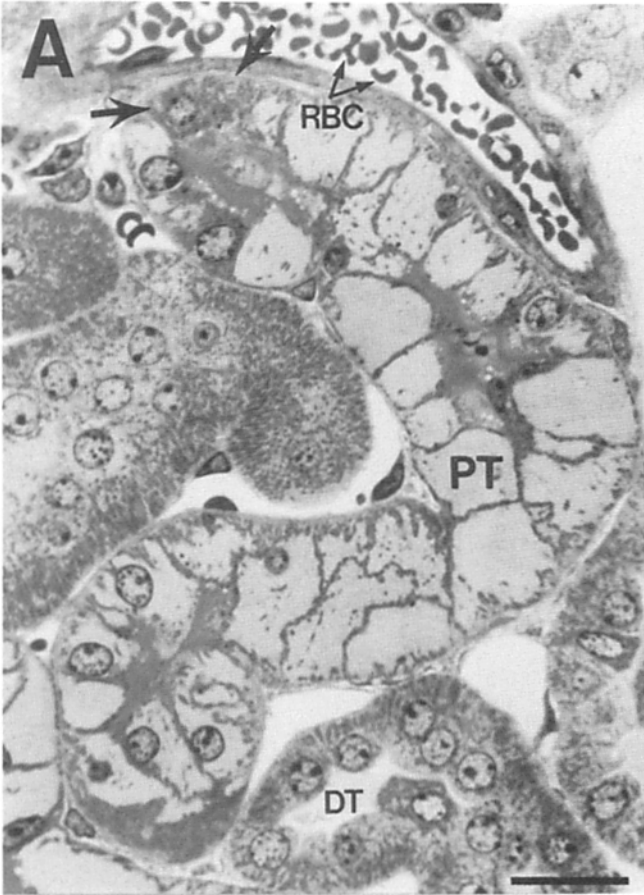
a goat polyclonal antibody to vimentin (ICN Immunobiologicals, Lisle, IL). Affinity-purified fluorescein- and rhodamine-conjugated antibodies specific for each of the primary antibodies were obtained from ICN Immunobiologicals.

Pulse Labeling of Proteins in Isolated Dorsal Root Ganglia

The right and left L4 and L5 dorsal root ganglia (DRG) were isolated from anesthetized mice (chloral hydrate 400 mg/kg, i.p.) and immediately placed in warm (37°C) DME. Newly synthesized proteins were labeled by incubating the DRG for 15 min at 37°C in 150 μl of methionine-free DME supplemented with 250 μCi of L-[35S]methionine. The DRG were then washed in medium lacking the radioactive label and frozen at −70°C. To analyze the proteins labeled, the DRG were lysed by homogenization in 0.5% SDS (wt/vol), 50 mM Tris, pH 6.8. Protein concentration was determined by the bicinchonic acid method (Smith et al., 1985) and the amount of radiolabel incorporated determined by TCA precipitation. Either equal TCA-insoluble counts or equal protein fractions were analyzed by SDS-PAGE from transgenic mice and nontransgenic littermates to determine whether there was increased NF-L synthesis in the transgenic samples.

In Situ Hybridization

In situ hybridization was performed following the method of Lewis and Cowan (1985a). Lumbar DRG were removed from anesthetized mice, fixed by immersion in 4% paraformaldehyde fixative, embedded in paraffin, and sectioned (8 μm). Sections were acetylated with acetic anhydride before hybridization with 35S-labeled NF-L cDNAs (Lewis and Cowan, 1985b). Slides were washed under low stringency conditions (150 mM NaCl, 15 mM Na-citrate, 50°C) dipped in Kodak NTB3 emulsion, and exposed for 5–10 d.

Morphological Analyses of Axonal Cross-sectional Area and Axonal NF Content

The sciatic nerves of anesthetized mice were exposed and fixed in situ with 5% glutaraldehyde. Nerve segments were excised, fixed by immersion in fixative for an additional 24 h, postfixed in osmium, dehydrated, and embedded in Epon. For analyses of axonal caliber, 1-μm thick light microscope sections were stained with toluidine blue. Axonal cross-sectional areas were measured in corresponding regions of sciatic nerves from transgenic and nontransgenic littermate animals using a Bioquant computer-based system (R. M. Biometrics, Inc., Nashville, TN). For electron microscopic analyses of axonal NF content, representative areas of axoplasm from age-matched transgenic and control nerve fibers were photographed at a magnification of 25,000. Photographs were printed at a final magnification of 62,500, and NF cross sections were counted by two of the authors (Hoffman and Cleveland).

Immunohistochemistry

DRG and kidney, fixed by intracardiac perfusion of anesthetized mice with 4% paraformaldehyde, were embedded in parraffin, and sectioned (8 μm). Tissue sections were deparaffinized, incubated for 1 h in 5% nonfat dehydrated milk, and then incubated for 24 h in a rabbit polyclonal anti–NF-L antibody (kindly provided by Dr. Gerry Shaw, University of Florida) used at a 1:200 dilution in 5% nonfat dehydrated milk. (The commercial monoclonal antibody to NF-L could not be used because it did not recognize NF-L in formalin-fixed tissue.) Sections were then washed, incubated for 1 h in goat anti–rabbit antibody (diluted 1:20), washed again, and finally incubated for 1 h in rabbit peroxidase-antiperoxidase. Development was performed with 0.05% diaminobenzidine tetrahydrochloride/0.01% hydrogen peroxidase (5 min). All washes and solutions were in 0.05 M Tris-buffered 0.9% saline, pH 7.6. All incubations were carried out at room temperature. Sections were coverslipped, examined by light microscopy, and photographed.

Results

To produce mice bearing NF-L transgenes that might express increased NF-L in axons, we initially chose to inject the 7-kb Hind III DNA fragment containing the mouse NF-L gene into one-cell mouse embryos. We marked the injected DNA with a 13-base insertion within the 5' untranslated region of the NF-L gene so that the RNA from this transgene (pNF-L[Bam]; Fig. 1 B; see also Monteiro and Cleveland, 1989) could be clearly distinguished from that transcribed from the maternal and paternal NF-L genes. The encoded transgene polypeptide was the authentic, wild-type NF-L subunit. Two transgenic founder mice were obtained (σNF-9 and ♀NF-16) and DNA blotting showed that each contained one to two copies of the complete NF-L gene (Fig. 2 A). Using S1 protection of RNA isolated from various tissues, transgenic F1 progeny from each founder were assayed for expression of the transgene. By choosing an end-labeled S1 probe that contained the linker sequence that we had placed in the 5' untranslated region of the transgene (the Hind III–Ava I fragment of pNF-L[Bam]; Fig. 1 B), this probe simultaneously reported the RNA levels of the transgene (a 183-base protected fragment extending from the site of labeling to the site of transcription initiation) and the endogenous NF-L genes (∼93-base fragment extending from the site of labeling to the site of linker insertion). In both founders, transgene RNA accumulated only in brain, but not in liver, kidney, heart, spleen, or muscle (see Fig. 2 B for σ NF-9). However, neither transgene was as highly expressed as the endogenous NF-L RNAs, with σNF-9 RNA accumulation ∼20% of the endogenous and ♀NF-16 RNA ∼3% of the endogenous. Since the transgene encodes a wild-type NF-L protein, we could not assay directly for accumulation of protein encoded by it; however, immunoblot analysis of total NF-L protein in brain tissue was not detectably different in transgenic animals compared with control littermates (data not shown).

Production of Transgenic Mice Containing the NF-L Gene under the Control of the MSV LTR Promoter

Previously, we demonstrated in transfection experiments that in cultured mouse L cells the NF-L gene was expressed ∼10–20-fold higher when the NF-L promoter was replaced with the strong LTR promoter from MSV (Monteiro and Cleveland, 1989). Thus, we reasoned that the MSV LTR might also be suitable to increase expression of the NF-L transgene in neurons of transgenic mice. While we were also concerned that this viral promoter would probably yield expression in a wide variety of cell types and that this might be detrimental to the survival of the transgenic animals, we nevertheless injected mouse embryos with the MSV-NF-L gene construct (see Fig. 1 C). We obtained 13 transgenic founder mice (from 48 born) which blot analysis revealed to contain from 1 to 300 copies of the MSV-NF-L transgene (data not shown). Indeed, a simple assay for transgenic

---

Figure 5. Accumulation of NF-L filaments in transgenic kidney. (A) Light micrograph of a 1-μm-thick plastic section of a kidney from mouse line MSV-NF-L-58 (stained with toluidine blue). Bar, 20 μm. (B) Nomarski image of a similar, but unstained section after incubation with a polyclonal antibody to NF-L followed by a secondary antibody conjugated to peroxidase. Bar, 20 μm. (C) Higher magnification view using electron microscopy. Bar, 5 μm. (D) The area delineated by the rectangle in C was further magnified to reveal a densely packed array of filaments. Bar, 0.5 μm. Arrows in A and B denote nearby proximal tubule cells adjacent to others that accumulate high amounts of NF-L. PT, proximal tubule; DT, distal tubule; RBC, red blood cell; N, proximal tubule cell nuclei.

animals emerged when an immunoblot survey of proteins from mouse tails revealed the presence of NF-L in all transgenic founders, but not in control mice. The level of NF-L expression in tail correlated to a certain degree with copy number but was always similar for littermates acquiring the same transmitted transgene(s) (data not shown). For example, transgene expression showed some dependence on copy number up to ~30 copies, but this relationship was not apparent at higher copy numbers and in some cases other factors clearly influenced expression.

To determine the pattern of transgene expression in different tissues, we used immunoblotting to examine whole cell proteins from a series of tissues from control or transgenic animals. Fig. 3 displays such an analysis for line MSV-NF-L-72. Of the tissues examined in control animals, NF-L was restricted to brain as expected; however, in transgenic tissues, NF-L accumulation was easily detectable by Coomassie staining of whole cell extracts of skeletal muscle or kidney. Quantitation of these findings by parallel immunoblotting of known amounts of partially purified neurofilaments revealed NF-L accumulation in these tissues to be ~2.5% of total cell protein. In heart, NF-L contributed 0.5% of cell protein, while little transgene expression was observable in liver or spleen. However, in brain NF-L did not accumulate to a level in excess of that in nontransgenic littermates.

With one notable exception, a parallel comparison of transgene RNA levels in the same tissues revealed a pattern similar to that found for accumulated NF-L protein (Fig. 3 E and F). The striking exception was brain where transgene RNAs were more abundant than endogenous NF-L mRNAs (Fig. 3 E and F, lanes B). For example, using S1 analysis and an end-labeled probe derived from the authentic NF-L gene, the endogenous NF-L RNA protected the probe to the start site of transcription while transgene RNAs (that diverge from the probe at the site of linker insertion) yielded two major protected fragments of 145 and 158 bases (Fig. 3 F). (These major transgene protected fragments are ~11 and ~24 bases larger than the 134 bases predicted, probably because of the failure of S1 to cleave efficiently within either of two GC-rich domains that lie just 5′ to the point of transgene RNA/probe DNA sequence divergence.) Inspection of the data revealed that transgene RNAs were ~20-fold more abundant than NF-L RNAs. Despite this, no increase in accumulated NF-L protein was detectable in brain (Fig. 3, C and D, lanes B). These results were not unique to the MSV-NF-L-72 line; similar relative levels of transgene RNA and protein levels were found in analyses of tissues from two other founder lines that express the transgene highly (MSV-NF-L-58 and MSV-NF-L-103) (not shown).

The failure of NF-L protein to accumulate in brain may have resulted from the transgene encoding an assembly-incompetent NF-L subunit which might have been specifically susceptible to degradation. To test this, we prepared primary cultures of cells enriched in fibroblasts derived from transgenic mice and determined the localization of NF-L by immunofluorescence light microscopy. An antibody to NF-L stained a filamentous array in almost all of the cells from transgenic cultures (Fig. 4 A), but none of those derived from nontransgenic littermates (not shown). In fact, double immunofluorescence revealed that NF-L coassembles with vimentin (Fig. 4 B), the endogenous IF that the fibroblasts constitutively express.

To confirm further that the transgene encoded assembly-competent molecules, we used light and electron microscopy to analyze the kidneys of MSV-NF-L-58, in which NF-L accumulated to 2.5% of cell protein. Sections obtained from transgenic kidneys showed that proximal tubule cells contained substantial levels of NF-L, which was easily observable by immunoperoxidase staining with the NF-L antibody (Fig. 5 B). No NF-L was observed in distal tubules or the surrounding cells—for example, red blood cells (Fig. 5 A), or in kidneys from control animals. In fact, in many affected tubule cells NF-L accumulation was to such a level that it was easily observable as lightly staining domains encompassing most of the cell cytoplasm (Fig. 5 A). Higher magnification views using electron microscopy more clearly revealed these large accumulations of NF-L within tubule cells (Fig. 5 C), while even higher magnifications revealed them to be comprised of massive arrays of densely packed filaments 8–10 nm in diameter (Fig. 5 D). The presence of these accumulations of filaments had no discernible effect on the longevity of the mice (the founder mice are now 2 y old). That such massive filament accumulation had no overt phenotypic consequence is probably because not all proximal tubules were affected. For example, morphologically normal tubule cells were found to lie adjacent to those most strongly accumulating NF-L (see arrows in Fig. 5 A, or the uneven immunostaining within an affected tubule in Fig. 5 B). Why only some of the tubule cells are affected is unknown.

The only obvious phenotypic consequence of expression of NF-L outside neurons was the formation of cataracts (Fig. 6 A). These were especially noticeable in the three lines of mice that most highly express the pMSV-NF-L transgene. Although we have not followed the levels of NF-L accumulated during development nor have we carefully monitored the onset of cataract formation, cataracts were correlated with the presence of NF-L polypeptides in the lens. For example, Coomassie blue staining of proteins separated by electrophoresis revealed a major 68-kD protein unique to transgenic animals (Fig. 6 B) and immunoblotting confirmed its identity as NF-L (Fig. 6 C). The immunoblot further revealed that the NF-L antibody reacted not only with the expected 68-kD NF-L polypeptide but also with a number of smaller polypeptides which we presume to be proteolysis products of the 68-kD polypeptide. Comparison of the Coomassie staining at the NF-L position with that of the 50–57-kD region containing vimentin revealed that NF-L must be at least fivefold more abundant than vimentin, the IF normally expressed in lens.

In view of NF-L accumulation in nonneuronal tissues, the failure of the transgene RNA to elevate NF-L in brain is surprising, but obviously cannot be the result of an inadvertent mutation in the transgene. Rather, it may indicate the presence of a posttranscriptional regulatory mechanism that acts to limit NF-L accumulation in some (and perhaps most) brain cells.

Expression of NF-L in Peripheral Sensory Neurons of Transgenic Mice

Although we did not detect any increase in accumulated NF-L protein in the brains of transgenic mice despite substantially increased NF-L mRNAs, we also examined NF-L accumulation in peripheral neurons. As a tissue rich in neurons, DRG
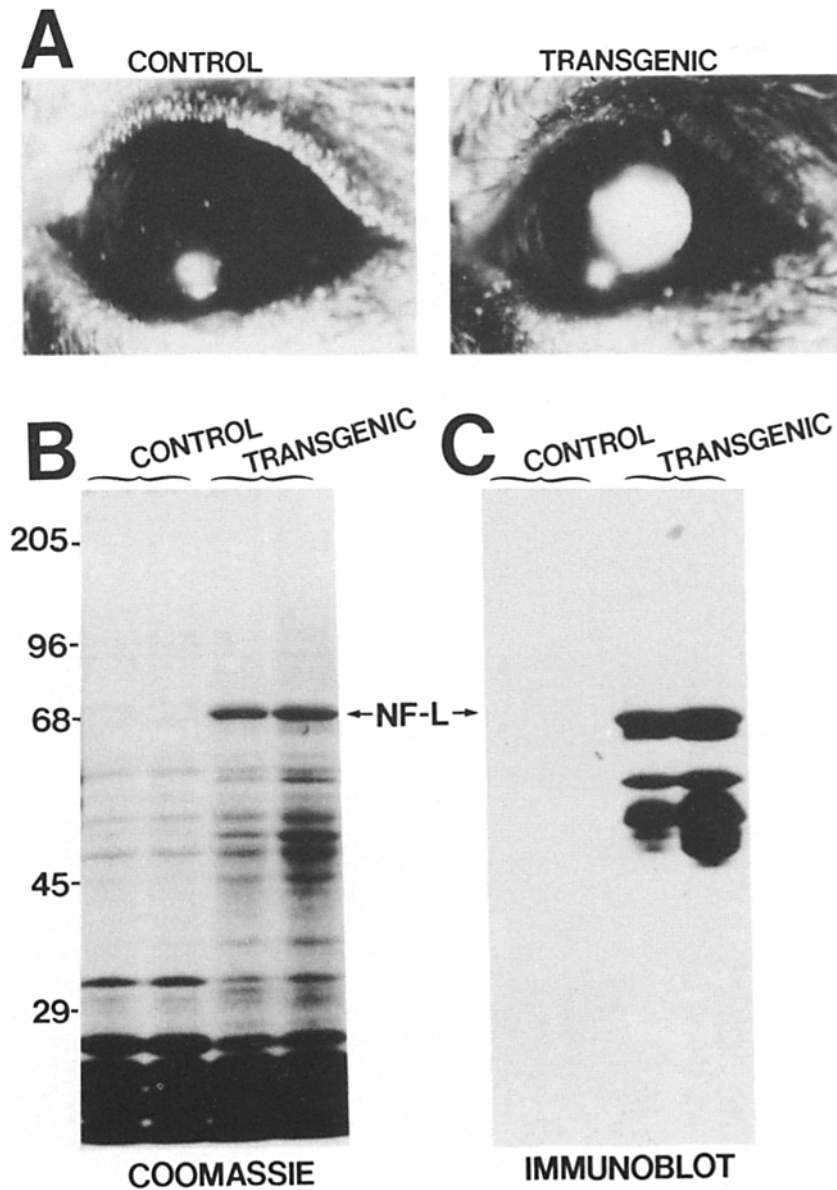
Figure 6. Cataract formation in eyes of mice expressing NF-L in lens. (*A*) Photographs of eyes of control and transgenic littermates of line MSV-NF-L-58 at ∼6 mo. (*B*) Coomassie-stained gel and (*C*) immunoblot of whole lens cell extracts of two control and two transgenic MSV-NF-L-58 animals. NF-L polypeptides were identified in *C* with the monoclonal antibody to NF-L.

were selected for further analysis. DRG contain the cell bodies of sensory neurons as well as axons ensheathed by Schwann cells, the myelin-forming cells of peripheral nerve. Each sensory neuron gives rise to a single axonal stem process, which bifurcates within the ganglion into a central axonal process that extends to the spinal cord (via the dorsal root) and a peripheral axonal process that extends into the peripheral nerve (the sciatic nerve, in the case of the L4 and L5 DRG analyzed in these studies). Neuronal protein synthesis takes place exclusively within the cell bodies, and newly synthesized cytoskeletal proteins, including NF-L, enter the axon where they are translocated towards the axon terminals at velocities of several millimeters per day via slow axonal transport (Hoffman and Lasek, 1975).

S1 nuclease analysis of NF-L mRNAs isolated from the DRG of line MSV-NF-L-58 revealed that there was about fivefold more transgene RNA than endogenous NF-L RNAs (Fig. 7 *A*, *DRG*). This was consistent with transgene expression in either the neurons or Schwann cells of the DRG, or

both. (RNA blotting revealed that the abundance of NF-M and NF-H mRNAs was comparable in DRG of transgenic and control animals [data not shown].) A similar analysis revealed the relative absence of either transgene or endogenous NF-L RNAs in sciatic nerve (Fig. 7 *A*, *NERVE*), which contains axons and Schwann cells, but not neuron cell bodies. (Axons lack ribosomes and mRNAs and cytoplasmic protein synthesis in neurons is thus confined to the cell body [Lasek et al., 1973].) These results suggested a high level of expression of the transgene within the neurons of the DRG.

To confirm the localization of transgene RNAs in neuronal cell bodies in DRG, we used in situ hybridization. For this, we used a probe that hybridized both to the transgene and to the endogenous NF-L mRNAs. This revealed prominent localization of NF-L mRNAs in neuron cell bodies (Fig. 8 *A*, *large arrows*), with little if any hybridization to adjacent Schwann cells (Fig. 8 *A*, *small arrows*). (Localization uniquely of MSV-NF-L transgene RNAs could not be achieved by in situ hybridization since the endogenous and transgene
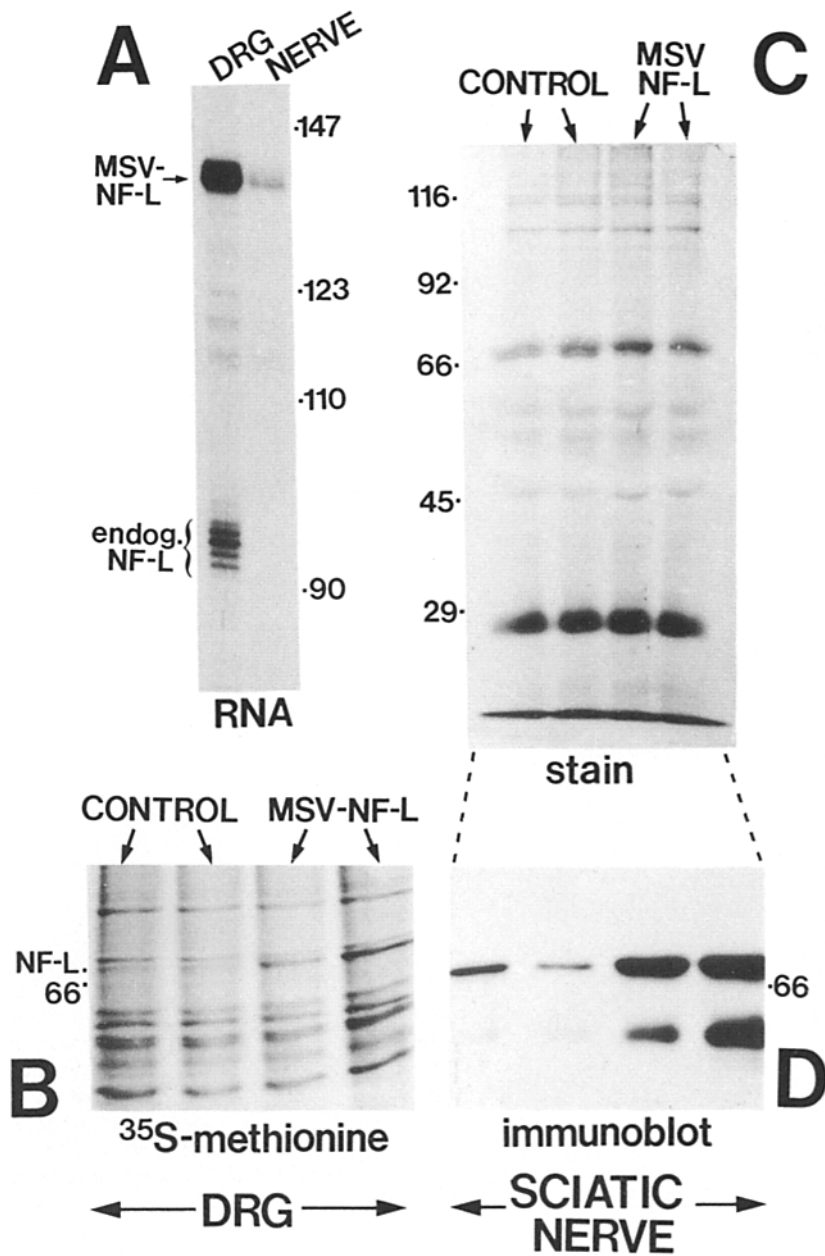
Figure 7. Increased expression of NF-L in DRG and sciatic nerves of MSV-NF-L transgenic mice. (*A*) RNA purified from DRG and sciatic nerves of MSV transgenic mice (MSV-NF-L-58) was analyzed for abundance of NF-L RNAs by S1 nuclease protection using the Ava I–Ava I fragment of pMSV-NF-L (end-labeled with ^{32}P) as the probe. Transgene RNAs are reported as a 140-base protected fragment; the endogenous NF-L genes yield 92–96-base protected fragments. (*B*) Isolated DRG from MSV-transgenic mice synthesize increased levels of NF-L. L4 and L5 DRG were isolated from two MSV-NF-L-58 transgenic mice and from two control nontransgenic littermates. The DRG were pulse labeled for 15 min with [^{35}S]methionine and the radioactive proteins separated by SDS-PAGE and analyzed by fluorography. (*C* and *D*) Protein lysates of sciatic nerves (10 μg in each lane) obtained from two control and two transgenic mice were separated by electrophoresis. *C* displays a gel stained with Coomassie blue; *D* displays an immunoblot analysis of a parallel gel probed with a monoclonal antibody to NF-L.

RNAs differ only in the 5′-most 35 bases and we were unable to detect a signal using this 35-base region of the transgene. Nevertheless, since the probe reported both endogenous and transgene NF-L RNAs localized only to neuronal cells and the transgene RNAs are fivefold more abundant in the DRG, we infer that the MSV-promoted NF-L transcripts must contribute at least five-sixths of the hybridization signal seen over the cell bodies of the neurons.) Further, the lack of in situ hybridization in regions of DRG enriched in Schwann cells and axons but lacking neuron cell bodies (lower region of Fig. 8 *A*) is consistent with the relative absence of NF-L RNAs in peripheral nerve (Fig. 7 *A*, *NERVE*), whose RNA content is contributed primarily by Schwann cells. Previous in situ hybridization studies have shown that these Schwann cells contain high levels of tubulin mRNAs (Hoffman, P. N., and D. W. Cleveland, unpublished observations) and thus the

lack of hybridization with the NF-L cDNA does not reflect limited access of probes to the regions of DRG tissue sections enriched in Schwann cells.

That transgene NF-L expression was absent in the Schwann cells and largely confined to the large neurons was further confirmed by localization of NF-L protein using a polyclonal antibody that recognizes NF-L in formalin-fixed tissue sections. (The mAb used for earlier immunoblot and immunofluorescence analyses did not recognize NF-L in formalin-fixed tissue.) As shown in Fig. 8 *B*, large neuronal cell bodies were intensely stained, with little or no detectable NF-L in Schwann cells or smaller neurons. While the antibody cannot distinguish between the endogenous and transgene NF-L, these results clearly demonstrate that if the transgene product is present at substantial levels, its accumulation must be restricted to these large neurons.
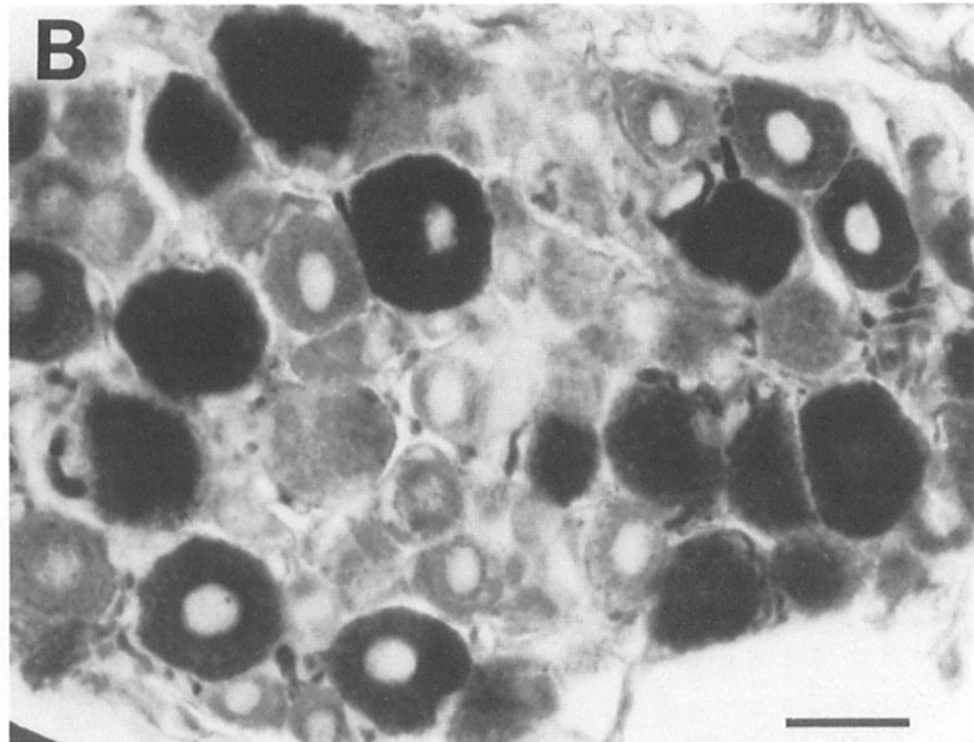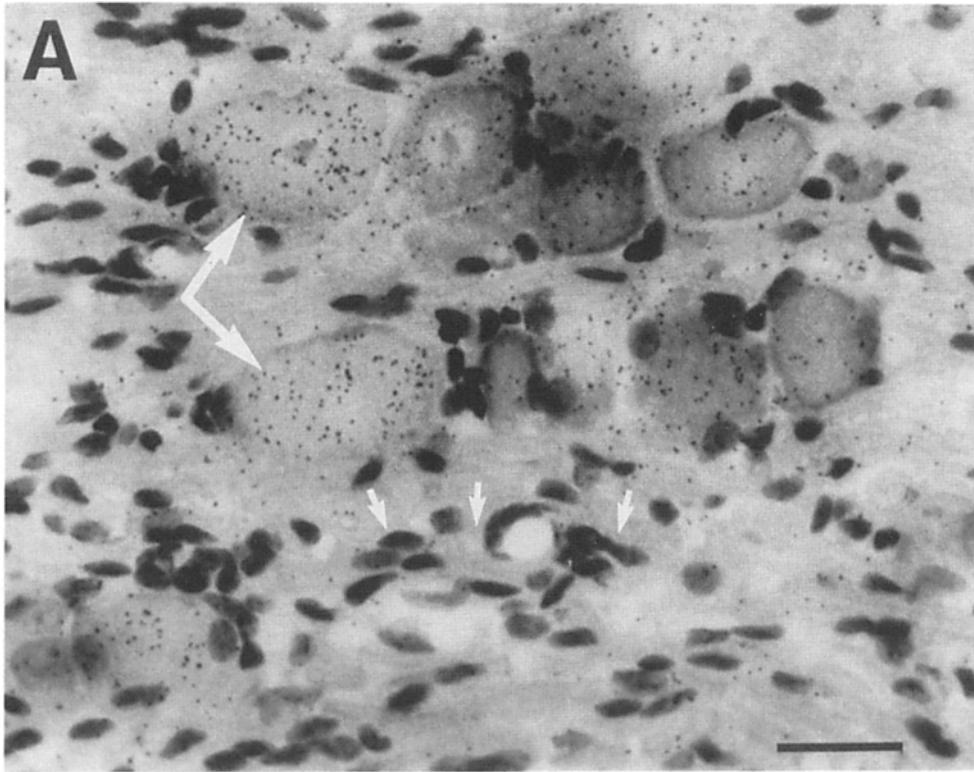
*Figure 8.* Localization of NF-L mRNAs and protein in transgenic sensory neurons. (*A*) In situ hybridization of ^{35}S-labeled cDNA that specifically hybridizes with NF-L mRNAs was performed on tissue sections containing lumbar sensory neurons from an animal expressing the pMSV-NF-L transgene. The autoradiogram was exposed for 5 d. Large arrows point to neuron cell bodies covered with silver grains. Small arrows point to areas enriched in Schwann cells. (*B*) Immunohistochemical localization of NF-L in transgenic sensory neurons. This formalin-fixed tissue was stained with a polyclonal antibody to NF-L. Bars, 25 μm.

We next determined whether comparable increases in NF-L synthesis were detectable in these DRG neurons that contain elevated levels of NF-L mRNAs. To do this, we isolated L4 and L5 DRG of transgenic animals and nontransgenic littermate controls. These were incubated with [^{35}S]methionine for 15 min to label newly synthesized proteins, which were then separated by SDS-PAGE and analyzed by fluorography. The pattern of newly synthesized proteins was identical in control and transgenic mice with the exception that in transgenic animals there was a clear elevation in a 68-kD polypeptide, which is the expected size of NF-L (see Fig. 7 *B*). This increase in the rate of synthesis of NF-L is compara-
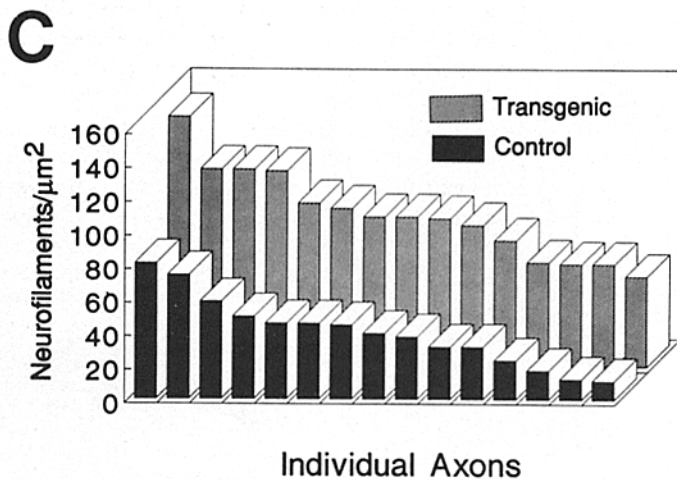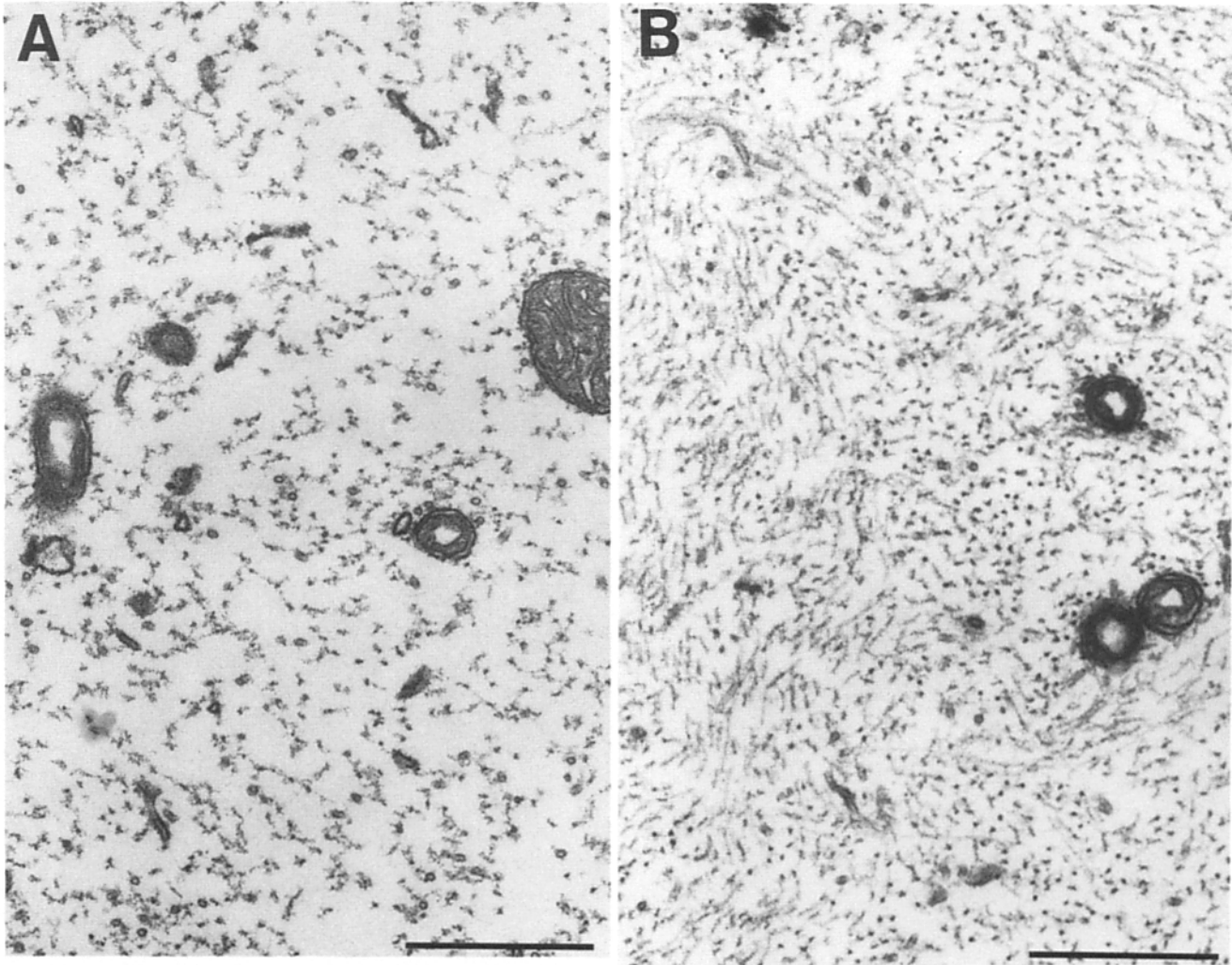
Figure 9. Increased NF density in transgenic axons. Electron micrographs compare representative areas of axoplasm in large myelinated nerve fibers of (A) a control and (B) a transgenic animal expressing pMSV NF-L. NF density is greater and the orientation of NF is more variable in transgenic as compared to control axons. Bars, 0.5 μm. (C) Quantitation of NF density in large myelinated nerve fibers of transgenic (light bars) and littermate control animals (dark bars). NF density is ranked from greatest to least for each group in order to facilitate comparison.
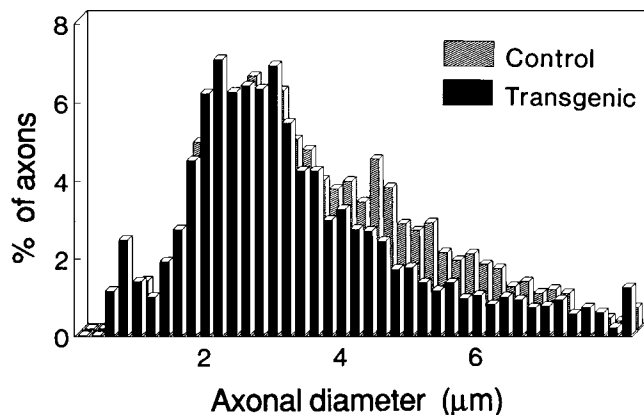
Figure 10. Comparison of mean axonal diameters in the sciatic nerves of control animals and transgenic animals expressing pMSV-NF-L. Axonal cross-sectional areas were measured using a computer-based system and mean diameters were calculated. Nerves were analyzed from two transgenic and two control animals; mean cross-sectional areas were measured for 2,525 control axons and 2,975 transgenic axons.

ble to the increase in NF-L RNAs, although the relatively low level of NF-L in control DRG precluded precise quantitation.

To test whether this increased rate of synthesis of NF-L in the neuron cell bodies resulted in increased levels of NF-L protein in axons, we analyzed the abundance of NF-L protein in the sciatic nerves of control and transgenic animals. Equal amounts of nerve extracts from two MSV-NF-L-58 transgenic animals and from two age-matched, littermate controls were immunoblotted for NF-L. Fig. 7 *C* shows the Coomassie stain of total nerve proteins and Fig. 7 *D* displays the corresponding NF-L immunoblot. Clearly, the transgenic samples contain substantially more NF-L (three to six times as much by densitometry). We have performed this experiment three times with six transgenic animals and have always observed a similar increase in NF-L content. Additional immunoblots of sciatic nerve proteins revealed that the levels of NF-M and NF-H subunits were comparable in transgenic and control animals (data not shown). It is highly likely that the increased abundance of NF-L in the sciatic nerves of transgenic animals reflects the axonal transport of increased amounts of NF-L in these nerve fibers (as opposed to stabilization of NF-L in transgenic nerves), although we have not yet directly tested this.

Characterization of Peripheral Axons of Transgenic Mice by Electron Microscopy

The morphological consequences of increased NF-L accumulation in the sciatic nerves of transgenic animals were analyzed by electron microscopy. Sciatic nerves isolated from adult (>6-mo-old) transgenic animals and from control nontransgenic littermates were fixed in 5% glutaraldehyde and embedded in Epon, and transverse sections were obtained and analyzed by electron microscopy. Comparison of the number of neurofilaments within both large and small caliber myelinated axons revealed a clear increase in the density of neurofilaments in the transgenic axons (compare Fig. 9, *A* and *B*). By carefully counting NF number, we determined the NF density to be 40 ± 20 NF/μm^2 in control

nerves and 88 ± 25 NF/μm^2 in transgenic axons. The relatively large SDs in NF density are, at least in part, the consequence of the difficulty in accurately counting NF, particularly in the transgenic axons where NFs are not uniformly aligned parallel to the longitudinal axis (e.g., Fig. 9 *B*). Since we did not count these nonaligned NFs, the actual differences in NF content between control and transgenic axons is actually greater. In any event, the measured 2.2-fold increased density of NF in transgenic axons was not accompanied by a detectable change in overall axonal caliber. Cross-sectional areas were measured for 5,500 axons and a histogram of the frequency of axonal diameters (calculated from the areas) revealed no significant change in axonal size (Fig. 10).

(It should be noted that sciatic nerve contains both sensory and motor axons, with the former arising from the DRG and the latter from the ventral spinal cord. The increase in NF density was seen in essentially all myelinated axons in the sciatic nerves of transgenic animals, indicating that NF-L content was increased in both sensory and motor fibers.)

Discussion

A series of preceding efforts had proposed a major role of NF gene expression in the control of axonal caliber. The most compelling evidence demonstrated that reductions in NF gene expression after axotomy are associated with decreased axonal caliber in large myelinated nerve fibers (Hoffman et al., 1987). Additional evidence comes from recent studies demonstrating that the radial growth of myelinated nerve fibers, which occurs during postnatal development, coincides temporally with the induction of NF gene expression in developing sensory neurons. This induction is absent in neurons giving rise to unmyelinated fibers, which contain relatively few NFs and do not undergo significant radial growth (Muma, N. A., and P. N. Hoffman, unpublished observations). Although the exact mechanisms by which NF content influences axonal caliber are unknown, these observations collectively support the hypothesis that NF gene expression is, at the least, a prerequisite for the radial growth of axons.

Previous studies have demonstrated a close correlation between axonal cross-sectional area and the axonal NF content of large myelinated nerve fibers (Friede and Samorajski, 1970; Weiss and Mayr, 1971; Berthold, 1978). Although modest differences in axonal NF density (~25%) have been reported among different populations of neurons (Price et al., 1988) and in different regions of small-caliber nerve fibers (Nixon and Logvinenko, 1986; Parhad et al., 1987), greater variations of NF density are not normally observed. The alterations in axonal NF content associated with somatofugal axonal atrophy (where NF content decreases) and with normal postnatal development (where NF content increases) correlate with changes in axonal cross-sectional area, rather than changes in NF density (Friede and Samorajski, 1970; Hoffman et al., 1984; Hoffman et al., 1985). Substantial increases in NF density are associated with the axonal abnormality induced by systemic intoxication with the neurotoxin iminodipropionitrile (Parhad et al., 1987), which selectively impairs NF transport (Griffin et al., 1978) and leads to a disorganization of axoplasm characterized by the malorientation of NF and the segregation of NF and microtu-

bules (Clark et al., 1980; Papasozomenos et al., 1981; Griffin et al., 1983). Like the iminodipropionitrile example, overexpression of wild-type NF-L yields not only an abnormal increase in NF density, but also disorganization of the axonal cytoskeleton.

Since the additional NF in the axons of transgenic animals are constructed primarily from NF-L, our findings demonstrate that an increase in filaments assembled primarily from NF-L has little effect on axonal caliber. Of course, we cannot exclude the possibility that a greater increase in NF-L accumulation would ultimately have resulted in altered axonal caliber, as happens in animals intoxicated with iminodipropionitrile. However, since NFs are normally composed of three different subunits, a simpler view is that an increase in NF-L alone may not result in the formation of filaments with the same properties as those composed of normal ratios of the three subunits.

Indeed, although NF-L can form filaments in the absence of the other subunits (Geisler and Weber, 1981; Liem and Hutchinson, 1982), it does not carry the extended carboxy-terminal tail shared by NF-M and NF-H (Sharp et al., 1982; Hirokawa et al., 1984; Hisanaga and Hirokawa, 1988), which in the case of NF-H appears to be associated NF cross-bridges (Hirokawa et al., 1984; Hisanaga and Hirokawa, 1988). It is possible that these cross-bridges play a critical role in the regulation of axonal caliber. In fact, the carboxy-terminal tail of NF-H is highly enriched in both charged amino acids and potential phosphorylation sites (Lees et al., 1988), suggesting that these cross-bridges may repel adjacent NF, thereby reducing NF density. The possible role of NF cross-bridges in the control of axonal caliber can now be explored by producing additional transgenic mice expressing higher levels of NF-M and NF-H subunits.

Two other transgenic founder mice obtained with the authentic NF-L gene promoter (pNF-L[Bam]) showed accumulation of NF-L RNAs restricted to tissue enriched in neurons (e.g., brain), similar to the endogenous NF-L gene. This indicates that most, if not all, of the elements that specify neuronal-specific expression must be contained within the 7-kb transgene fragment. Although we have not shown it directly, we assume that expression of the pNF-L(Bam) transgene is restricted to neurons based on the work of Julien et al. (1987) who demonstrated by in situ hybridization that expression of a human NF-L transgene contained on a 21.5-kb genomic DNA fragment was localized to neurons. Further, Byrne and Ruddle (1989) had previously demonstrated that the 1.5-kb segment of the mouse NF-L gene just 5' to transcription initiation was sufficient to yield brain-specific expression of a marker gene, but they could not determine the level of expression. Using the same presumptive NF-L promoter domain, we find transgene RNAs at a level 20% of the endogenous NF-L mRNAs in brain. Since NF-L RNA is moderately abundant, this indicates that use of the NF-L controlling sequences should produce a relatively high level of transgene expression targeted to most (and perhaps all) neurons.

MSV LTR–promoted transgenes produced very high expression of NF-L in various tissues, including many where NFs are not normally expressed. Somewhat surprisingly, NF-L accumulated to as much as 2–3% of total cell protein in tissues like kidney and skeletal muscle, and 0.5% in heart, and yet it had no catastrophic effect on the function of these tissues nor did it affect mouse development or survival. (The

founder mice are now 2 yr old.) This may at first seem surprising since NF-L is normally expressed only in postmitotic neurons. The combination of its unique expression in neurons and its extreme insolubility initially suggested that inappropriate expression of NF-L might be detrimental to continuing mitosis. However, using DNA transfection of cultured cells we showed that NF-L could accumulate to be the most abundant cellular protein without affecting cell growth (Monteiro and Cleveland, 1989). Our current results extend this finding to a true in vivo situation: inappropriate expression of NF-L did not affect the viability of the many different mitotic cell types in these transgenic mice. Furthermore, we have observed massive accumulation of NF-L filaments in kidney of transgenic mice without any obvious effect on longevity. The only phenotypic effect we have observed upon nontissue-specific expression of NF-L is the formation of cataracts. Capetanaki et al. (1989) also observed cataracts in transgenic mice that expressed the chicken vimentin gene in lens and concluded that vimentin expression specifically prevented normal lens cell differentiation, ultimately resulting in cataract formation. An alternative explanation that may in fact explain both that observation and ours is that the lens has a very restricted tolerance for expression of "foreign" proteins without the phenotypic consequence of cataract formation.

One set of previous transgenic animals had demonstrated that MSV directed transgene expression at high levels in lens and testis, with lower levels in brain and kidney (Khillan et al., 1987). Our findings confirm that the MSV promoter can be used to yield extraordinarily high levels of transgene expression albeit in a different set of tissues than seen earlier. Specifically, we have now documented MSV-directed expression in tissues rich in neurons. Although lower than that seen in the highest expressing tissues, transgene expression in DRG and in brain was nevertheless substantial enough that MSV-NF-L RNAs were 5–20-fold higher than those from the endogenous NF-L genes. Since a similar pattern was observed in three different transgenic lines, this suggests that the MSV LTR may also be of general use to force high level expression of selected gene products within neurons.

An unexpected finding was that the increase of MSV-promoted NF-L RNAs in the brains of transgenic mice did not result in a similar increase in NF-L protein. This clearly indicates the presence of posttranscriptional mechanisms that maintain the level of NF-L protein in brain. With the current mice we can not easily pursue the actual mechanism involved since the transgene translation product is identical to the endogenous NF-L. But in any event, the present data suggest interesting and novel posttranscriptional regulation of NF-L in the central nervous system.

References

Berthold, C. H. 1978. Morphology of normal peripheral axons. *In* Physiology and Pathobiology of Axons. S. G. Waxman, editor. Raven Press, New York. 3–63.

Byrne, G. W., and F. H. Ruddle. 1989. Multiplex gene regulation: a two tiered approach to transgene regulation in transgenic mice. *Proc. Natl. Acad. Sci. USA.* 86:5473–5477.

Capetanaki, Y., S. Smith, and J. P. Heath. 1989. Overexpression of the vimentin gene in transgenic mice inhibits normal lens cell differentiation. *J. Cell Biol.* 109:1653–1664.

Chirgwin, J. M., A. E. Przbyla, R. J. MacDonald, and W. J. Rutter. 1979. Isolation of biologically active ribonucleic acid from sources enriched in ribonuclease. *Biochemistry.* 18:5294–5299.

Clark, A. W., J. W. Griffin, and D. L. Price. 1980. The axonal pathology in chronic IDPN intoxication. *J. Neuropathol. Exp. & Neurol.* 39:42–55.

Denhardt, D. T. 1966. A membrane-filter technique for the detection of complementary DNA. *Biochem. Biophys. Res. Commun.* 23:641–646.

Dretzen, G., M. Bellard, O. Sassone-Corsi, and P. Chambon. 1981. A reliable method for the recovery of DNA fragments from agarose and acrylamide gels. *Anal. Biochem.* 112:295–298.

Franke, W. W. 1987. Nuclear lamins and cytoskeletal intermediate filament proteins: a growing multigene family. *Cell.* 48:3–4.

Friede, R. L., and T. Samorajski. 1970. Axon caliber related to neurofilaments and microtubules in sciatic nerve fibers of rats and mice. *Anat. Rec.* 167:379–388.

Geisler, N., and K. Weber. 1981. Self-assembly in vitro of the 68,000 molecular weight component of the mammalian neurofilament triplet proteins into intermediate-size filaments. *J. Mol. Biol.* 151:565–571.

Geisler, N., and K. Weber. 1986. Structural aspects of intermediate filaments. *In* Cell and Molecular Biology of the Cytoskeleton. J. W. Shay, editor. Plenum Press, New York. 41–68.

Geisler, N., E. Kaufmann, S. Fischer, U. Plessmann, and K. Weber. 1983. Neurofilament architecture combines structural principles of intermediate filaments with carboxy-terminal extensions increasing in size between triplet proteins. *EMBO (Eur. Mol. Biol. Organ.) J.* 2:1295–1302.

Griffin, J. W., K. E. Fahnestock, D. L. Price, and P. N. Hoffman. 1983. Microtubule-neurofilament segregation produced by β,β'-iminodipropionitrile: evidence for the association of fast axonal transport with microtubules. *J. Neurosci.* 3:557–566.

Griffin, J. W., P. N. Hoffman, A. W. Clark, P. T. Carroll, and D. L. Price. 1978. Slow axonal transport of neurofilament proteins: impairment by β,β'-iminodipropionitrile administration. *Science (Wash. DC).* 202:633–635.

Hirokawa, N., M. A. Glicksman, and M. B. Willard. 1984. Organization of mammalian neurofilament polypeptides within the neuronal cytoskeleton. *J. Cell Biol.* 98:1523–1536.

Hisanaga, S.-I., and N. Hirokawa. 1988. Structure of the peripheral domains of neurofilaments revealed by low angle rotary shadowing. *J. Mol. Biol.* 202:297–305.

Hoffman, P. N., and R. J. Lasek. 1975. The slow component of axonal transport: identification of the major structural polypeptides of the axon and their generality among mammalian neurons. *J. Cell Biol.* 66:351–366.

Hoffman, P. N., J. W. Griffin, and D. L. Price. 1984. Control of axonal caliber by neurofilament transport. *J. Cell Biol.* 99:705–714.

Hoffman, P. N., G. W. Thompson, J. W. Griffin, and D. L. Price. 1985. Changes in neurofilament transport coincide temporally with alterations in the caliber of axons in regenerating motor fibers. *J. Cell Biol.* 101:1332–1340.

Hoffman, P. N., D. W. Cleveland, J. W. Griffin, P. W. Landes, N. J. Cowan, and D. L. Price. 1987. Neurofilament gene expression: a major determinant of axonal caliber. *Proc. Natl. Acad. Sci. USA.* 84:3472–3476.

Julien, J.-P., and W. E. Mushynski. 1983. The distribution of phosphorylation sites among identified proteolytic fragments of mammalian neurofilaments. *J. Biol. Chem.* 258:4019–4025.

Julien, J.-P., I. Tretjakoff, L. Beaudet, and A. Peterson. 1987. Expression and assembly of a human neurofilament protein in transgenic mice provide a novel neuronal marking system. *Genes & Dev.* 1:1085–1095.

Julien, J.-P., F. Cote, L. Beaudet, M. Sidky, D. Flavell, F. Grosveld, and W. Mushynski. 1988. Sequence and structure of the mouse gene coding for the largest neurofilament subunit. *Gene.* 68:307–314.

Khillan, J. S., M. K. Oskarsson, F. Propst, T. Kuwabara, G. F. Vande Woude and H. Westphal. 1987. Defects in lens fiber differentiation are linked to c-mos overexpression in transgenic mice. *Genes & Dev.* 1:1327–1335.

Laemmli, U. K. 1970. Cleavage of structural proteins during the assembly of the head of bacteriophage T4. *Nature (Lond.).* 227:680–685.

Lasek, R. J., C. Dabrowski, and R. Nordlander. 1973. Analysis of axoplasmic RNA from invertebrate giant axons. *Nat. New Biol.* 244:162–165.

Lees, J. F., P. S. Shneidman, S. F. Skuntz, M. J. Carden, and R. A. Lazarini. 1988. The structure and organization of the human heavy neurofilament subunit (NF-H) and the gene encoding it. *EMBO (Eur. Mol. Biol. Organ.) J.* 7:1947–1955.

Lendahl, U., L. B. Zimmerman, and R. D. G. McKay. 1990. CNS stem cells express a new class of intermediate filament protein. *Cell.* 60:585–595.

Levy, E., R. H. K. Liem, P. D'Eustachio, and N. J. Cowan. 1987. Structure and evolutionary origin of the gene encoding mouse NF-M, the middle-molecular-mass neurofilament protein. *Eur. J. Biochem.* 166:71–77.

Lewis, S. A., and N. J. Cowan. 1985a. Temporal expression of mouse glial fibrillary acid protein mRNA studied by a rapid in situ hybridization procedure. *J. Neurochem.* 45:913–919.

Lewis, S. A., and N. J. Cowan. 1985b. Genetics, evolution, and expression of the 68,000 mol. wt. neurofilament protein: isolation of a cloned cDNA probe. *J. Cell Biol.* 100:843–850.

Lewis, S. A., and N. J. Cowan. 1986. Anomalous placement of introns in a member of the intermediate filament multigene family: an evolutionary conundrum. *Mol. Cell. Biol.* 6:1529–1534.

Liem, R. K. H., and S. B. Hutchinson. 1982. Purification of individual components of the neurofilament triplet: filament assembly from the 70,000 dalton subunit. *Biochemistry.* 21:3221–3226.

Lopata, M. A., and D. W. Cleveland. 1987. In vivo microtubules are copolymers of available β-tubulin isotypes: localization of each of six vertebrate β-tubulin isotypes using polyclonal antibodies elicited by synthetic peptide antigens. *J. Cell Biol.* 105:1707–1720.

Minami, Y., and H. Sakai. 1985. Dephosphorylation suppresses the activity of neurofilament to promote tubulin polymerization. *FEBS (Fed. Eur. Biochem. Soc.) Lett.* 185:239–242.

Monteiro, M. J., and D. W. Cleveland. 1989. Expression of NF-L and NF-M in fibroblasts reveals coassembly of neurofilament and vimentin subunits. *J. Cell Biol.* 108:579–593.

Myers, M. W., R. A. Lazzarini, V. M. Y. Lee, W. W. Schlaepfer, and D. L. Nelson. 1987. The human mid-size neurofilament subunit: a repeated protein sequence and the relationship of its gene to the intermediate filament gene family. *EMBO (Eur. Mol. Biol. Organ.) J.* 6:1617–1626.

Nixon, R. A., and K. B. Logvinenko. 1986. Multiple fates of newly synthesized neurofilament proteins: evidence for a stationary neurofilament network distributed nonuniformly along axons of retinal ganglion cell neurons. *J. Cell Biol.* 102:647–659.

Papasozomenos, S. C. H., L. Autilio-Gambetti, and P. Gambetti. 1981. Reorganization of axoplasmic organelles following β,β'-iminodipropionitrile administration. *J. Cell Biol.* 91:866–871.

Parhad, I. M., A. W. Clark, and J. W. Griffin. 1987. Effect of changes in neurofilament content on caliber of small axons: the iminodipropionitrile model. *J. Neurosci.* 7:2256–2263.

Price, R. L., P. Paggi, R. J. Lasek and M. J. Katz. 1988. Neurofilaments are spaced randomly in the radial dimensions of axons. *J. Neurocytol.* 17:55–62.

Sharp, G. A., G. Shaw, and K. Weber. 1982. Immunoelectron microscopic localization of the three neurofilament triplet proteins along neurofilaments of cultured dorsal root ganglion neurones. *Exp. Cell Res.* 137:403–413.

Smith, P. K., P. I. Krohn, G. T. Hermanson, A. K. Mallia, F. H. Gartner, M. D. Provenzaus, E. K. Fujimoto, N. M. Goeke, B. J. Olson, and D. C. Klenk. 1985. Measurement of protein using bicinchonic acid. *Anal. Biochem.* 150: 76–85.

Southern, E. M. 1975. Detection of specific sequences among DNA fragments separated by gel electrophoresis. *J. Mol. Biol.* 98:503–517.

Steinert, P. M., and D. R. Roop. 1988. Molecular and cellular biology of intermediate filaments. *Annu. Rev. Biochem.* 57:593–625.

Weiss, P. A., and R. Mayr. 1971. Organelles of neuroplasmic ("axonal") flow: neurofilaments. *Proc. Natl. Acad. Sci. USA.* 68:846–850.